Agricultural and Forest Meteorology 307 (2021) 108501

Contents lists available at ScienceDirect

Agricultural and Forest Meteorology

journal homepage: www.elsevier.com/locate/agrformet

Assessment of the inverse dispersion method for the determination of methane emissions from a dairy housing

Marcel Bühler [a,b,c,*], Christoph Häni [a], Christof Ammann [d], Joachim Mohn [e], Albrecht Neftel [f], Sabine Schrade [g], Michael Zähner [g], Kerstin Zeyer [e], Stefan Brönnimann [b,c], Thomas Kupper [a]

[a] School of Agricultural, Forest and Food Sciences HAFL, Bern University of Applied Sciences, Länggasse 85, 3052 Zollikofen, Switzerland
[b] Oeschger Centre for Climate Change Research, University of Bern, Hochschulstrasse 4, 3012 Bern, Switzerland
[c] Institute of Geography, University of Bern, Hallerstrasse 12, 3012 Bern, Switzerland
[d] Climate and Agriculture Group, Agroscope, Reckenholzstrasse 191, 8046 Zürich, Switzerland
[e] Laboratory for Air Pollution/Environmental Technology, Empa, Überlandstrasse 129, 8600 Dübendorf, Switzerland
[f] Neftel Research Expertise, 3033, Wohlen bei Bern, Switzerland
[g] Ruminants Research Unit, Agroscope, Tänikon 1, 8356 Ettenhausen, Switzerland

ARTICLE INFO

Keywords:
GasFinder3
Open-path tunable diode laser
Backward Lagrangian stochastic
Inhouse tracer ratio method
Uncertainty analysis
Enteric fermentation

ABSTRACT

Methane (CH_4) emissions from dairy housings, mainly originating from enteric fermentation of ruminating animals, are a significant source of greenhouse gases. The quantification of emissions from naturally ventilated dairy housings is challenging due to the spatial distribution of sources (animals, housing areas) and variable air exchange. The inverse dispersion method (IDM) is a promising option, which is increasingly used to determine gaseous emissions from stationary sources, as it offers high flexibility in the application at reasonable costs. We used a backward Lagrangian stochastic model combined with concentration measurements by open-path tunable diode laser spectrometers placed up- and downwind of a naturally ventilated housing with 40 dairy cows to determine the CH_4 emissions. The average emissions per livestock unit (LU) were 317 (±44) g LU^{-1} d^{-1} and 267 (±43) g LU^{-1} d^{-1} for the first and second campaign, in September – October and November – December, respectively. For each campaign, inhouse tracer ratio measurements (iTRM) were conducted in parallel during two subperiods. For simultaneous measurements, IDM showed average emissions which were lower by 8% and 1% than that of iTRM, respectively, for the two campaigns. The differences are within the uncertainty range of any of the two methods. The IDM CH_4 emissions were further analysed by wind direction and atmospheric stability and no differences in emissions were found. Overall, IDM showed its aptitude to accurately determine CH_4 emissions from dairy housings or other stationary sources if the site allows adequate placement of sensors up- and downwind in the prevailing wind direction. To acquire reliable emission data, depending on the data loss during measurements due to quality filtering or instrument failure, a measuring time of at least 10 days is required.

1. Introduction

Global emissions of greenhouse gases from the livestock sector are estimated at 7100 Tg CO_2-eq per year, which corresponds to 14.5% of the anthropogenic GHG emissions (Gerber, 2013). Approximately 3100 Tg CO_2-eq or 44% of livestock emissions are due to the release of methane (CH_4) with the main share provided by cattle (2000 Tg CO_2-eq per year) (Gerber, 2013). CH_4 in the livestock sector is mainly produced through enteric fermentation in the digestive tract of livestock animals (Niu et al., 2018) and to a smaller extent during manure management, which in temperate regions accounts for about 15-20% of CH_4 emissions (Petersen, 2018), and includes the livestock building, manure processing and storage (Gerber 2013). For the period 2008-2017, Saunois et al. (2020) estimated total emissions for enteric fermentation and manure management at 111 Tg CH_4 yr^{-1} or 2775 Tg CO_2-eq which corresponds to one third of the global anthropogenic CH_4 emissions (366 Tg CH_4 yr^{-1}).

Loose housing systems in a naturally ventilated building are becoming the most common housing type for cattle in Switzerland (Kupper et al., 2015). CH_4 emissions from this system for dairy cows

* Corresponding author.
E-mail address: marcel.buehler@bfh.ch (M. Bühler).

https://doi.org/10.1016/j.agrformet.2021.108501
Received 1 December 2020; Received in revised form 29 April 2021; Accepted 29 May 2021
Available online 15 June 2021

were found to vary over a large range (Poteko et al., 2019). The quantification of gaseous emissions from naturally ventilated livestock buildings is challenging due to the spatial distribution of sources (animals, housing areas) and variable air exchange rates.

The inverse dispersion method (IDM) is a promising option for emission determination from stationary sources such as livestock housings, without the need to access the buildings. It combines concentration measurements up- and downwind of the source with turbulence measurements and a dispersion model to quantify the emission strength. Backward Langrangian stochastic (bLS) models are most commonly used in the IDM approach, but simple Gaussian plume models or complex fluid dynamics models are also possible (Harper et al., 2011; Sonderfeld et al., 2017). The IDM has been successfully applied to estimate emissions e.g. from whole farms (including stationary sources such as animal housings and manure stores) (Flesch et al., 2005; Flesch et al., 2009; McGinn et al., 2006; VanderZaag et al., 2008), animal production buildings (Harper et al., 2010), feedlots (Bai et al., 2017; Flesch et al., 2007; McGinn et al., 2007; McGinn et al., 2016), grazing cattle (Laubach et al., 2013; Laubach et al., 2014) and manure stores (Flesch et al., 2013). In an experiment with controlled CH_4 release in an animal housing, a recovery rate between 0.93 and 1.03 was achieved for IDM at a fetch between 10 and 25 times the housing height (Gao et al., 2010). These studies have highlighted the flexibility in the application of IDM for farm scale measurements.

In contrast to the current published studies with IDM application, livestock farms in Switzerland are often located in hilly terrain with substantial topographical variation in nearby surroundings. The prevailing micrometeorological conditions are often associated with low wind speed and unsteady wind directions. Furthermore, the average Swiss dairy farm is relatively small, housing only 22 dairy cows on average (Federal Statistical Office, 2020) and there are often neighbouring farms with potentially confounding CH_4 emissions in the vicinity of the target source. This leads to a small CH_4 concentration gradient up- and downwind of the source. All these factors make a successful application of the IDM challenging.

In this study, we investigate the applicability and performance of the IDM for a naturally ventilated dairy housing in eastern Switzerland as a relatively weak CH_4 source where variable and unsteady wind conditions prevail. The dependence of the IDM results on micrometeorological conditions and the housing dimensions, influencing the turbulence at the positions of the measuring devices, are analysed. This is necessary, as the bLS model assumes a flat topography with emissions released at ground level. The average CH_4 emission obtained by the IDM are compared to independent simultaneous measurements by an in-house tracer ratio method (iTRM).

2. Material and methodology

2.1. Experimental site and periods

2.1.1. Geographical location

Measurements were conducted at a naturally ventilated dairy housing in Aadorf, Switzerland (47.489175° N, 8.919663° E) which is an experimental facility of Agroscope (Mohn et al., 2018). The housing is built on a small plain that extends > 1 km in southwest direction and 220 m in northeast direction (main two wind directions). In the northeast, the plain terrain is followed by a descending slope of about 9%. Next to the dairy housing towards the northwest, outside the main wind directions, there is a building and some trees, which exceed 10 m height (Fig. 1). 200 m westward, a small forest is situated. Apart from the associated slurry pit at the southwest side of the housing (Fig. 1), no other potential CH_4 sources were present in close vicinity of the building. However, within a radius of 600 m of the dairy housing there are three other livestock housings (280 m south, 370 m east, 570 m west) and temporary grazing cattle and sheep (200 m northwest, 380 m east, 100-500 m north).

2.1.2. Experimental dairy housing and livestock

The dairy housing is 50 m long, 25 m wide and 5 m and 8.5 m high in the southwest and northeast side, respectively. It has a mono-pitched roof with the slope towards southwest. The main building axis is oriented perpendicular to the prevailing wind direction (Fig. 1). The housing consists of two experimental compartments for 20 cows each with cubicles equipped with straw mattresses and solid floors with a common rubber mat. The layout of the functional areas is further described in Poteko et al. (2018). In the centre section between the two compartments, the milking parlour and waiting area as well as technical installations, office and analytics are placed. The feeding aisles and cubicle access areas were equipped with stationary scrapers, which removed the dung 12 times per day to cross channels. These cross channels were emptied in around 8 to 12 days intervals into the two separated below-ground slurry pits at the southwest side situated outside of the building. The slurry pits are covered with a concrete ceiling that contains eight openings (each around 0.8 m^2). The total volume and slurry surface of the slurry pits are 252.2 m^3 and 127 m^2, respectively.

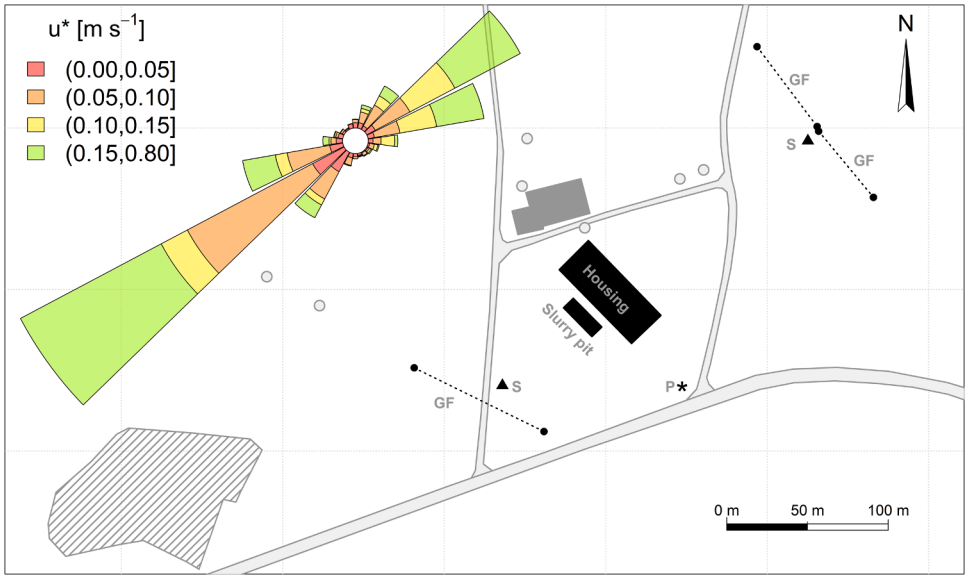

Fig. 1. Schematic overview of the measuring location with a wind rose. The wind rose indicates the frequency of occurrence of wind directions and the friction velocity u* in each wind direction sector. The large black rectangle is the dairy cattle housing with the underground slurry pit on the southwest side. Filled black circles indicate positions of GasFinder (GF) sensors and retroreflectors with the dashed line representing the measuring path. The black triangles mark the position of the sonic anemometers (S). The inlet for the iTRM background measurements (P) is denoted as asterisk. Further, trees (grey circles), forest area (hatched polygon), a building (dark grey polygon) and the streets (light grey) are drawn.

The experimental compartments are naturally ventilated without thermal insulation and with flexible curtains as facades. Management routines such as milking (05:30 and 16:30) and dung removal with stationary scrapers were the same in both measuring campaigns. Due to nutrition trials, which were carried out in parallel using the two groups of 20 dairy cows each, the diets during the iTRM measurements phases consisted of (i) hay, maize pellets and pellets of a mixture of maize and beans, or (ii) grass silage, maize silage and hay in compartment one and two, respectively. In addition, concentrates rich in energy and protein were allocated according to milk yield and body condition by an automatic feeder individually. Between the two iTRM measurements in each campaign, the rations (i) and (ii) were interchanged between the groups in the two compartments with prior phases allowing the cows to gradually adapt to the new diet. The silage-free diet (i) was provided twice per day (05:00 and 15:30) and the silage diet (ii) once per day (15:30). The cows had access to the fresh feed after each milking. The feed was automatically moved towards the cows 18 times a day.

During both measuring periods 40 lactating cows of Brown Swiss and Swiss Fleckvieh breeds were housed in the dairy housing for emission measurements (Table 1). The cows had no access to pasture or to the outdoor exercise areas during the measurements.

2.1.3. Measurement campaigns

Measurements were conducted during two campaigns in 2018. The first campaign lasted for 36 days from 17 September to 23 October with iTRM measurements conducted for two subperiods of eight days from 24 September to 02 October and 15 October to 23 October. The second campaign comprised 23 days of measurements from 24 November to 17 December with iTRM measurements divided into two subperiods of four days conducted from 26 November to 30 November and 11 December to 15 December.

The two campaigns were planned as two individual campaigns to reflect varying meteorological conditions which turned out to be substantially different in the first and second campaign (Section 3). Additionally, the herd composition was not identical (Table 1). Therefore, in the following we differentiate between the two campaigns.

2.2. Inverse dispersion method

2.2.1. Concept

IDM is a micrometeorological method to determine gaseous emissions from a spatially limited source of known area. The difference between measured concentrations upwind (C_{UW}, background concentration) and downwind (C_{DW}) of the source is proportional to the total emission rate Q between upwind and downwind concentration measurement (Eq. 1).

$$C_{DW} - C_{UW} = D * Q \quad (1)$$

The dispersion factor D is determined from measured turbulence characteristics by a dispersion model. Here, the bLS model described in Flesch et al. (2004) was used. With the modelled D_{bLS} [s m^{-3}] values and the measured concentrations C_{DW} and C_{UW} [mg m^{-3}] the emission flux Q [mg s^{-1}] can be calculated (Eq. 2).

$$Q = \frac{C_{DW} - C_{UW}}{D_{bLS}} \quad (2)$$

The line-integrating concentration measurements (Section 2.2.2) were approximated by a series of point sensors with a 1 m spacing along the path length. For each sensor and emission interval, 250,000 backward trajectories were calculated and analysed for touchdowns within the source area. The simulations were done with the R package bLSmodelR (Häni et al., 2018), available at https://github.com/ChHaeni/bLSmodelR.

2.2.2. Methane concentration measurements

For the concentration measurements, open-path tunable diode laser spectrometers (GasFinder3-OP, Boreal Laser Inc., Edmonton, Canada) and retroreflectors with seven corner cubes were utilised. The GasFinders measure at a frequency range of 0.3 - 1 Hz. The sensors and heated retroreflectors were connected to the power grid. The CH_4 concentration measurements were corrected for temperature and pressure influences using device specific relationships determined by Boreal Laser after construction (Boreal Laser Inc., 2018).

Concentration data was used only if the 'received power' of the reflected incoming laser beam was in the range of 200 to 2500 μW for two of the GasFinders. Due to erroneous concentration measurements when 'received power' was low, a more restrictive threshold of 400 to 2500 μW was used for the third GasFinder. For all three GasFinders the threshold for the goodness of fit between the sample and the calibration waveform quantified as R2 was 98%. The 0.3 - 1 Hz data were then averaged to 30 min intervals and periods with a data coverage of less than 75% (22.5 min) were removed. The three GasFinders were intercalibrated between the two campaigns and further, to relate measurements to international scales (WMO X2004A), the data was corrected to match independent background measurements from a cavity ring-down spectrometer (CRDS, model G2301, Picarro Inc., Santa Clara, USA) with an inlet 30 m southeast of the housing (Fig. 1). The interquartile range of the background concentration was 2.04 – 2.45 ppm. The interquartile range of the concentration difference (downwind – background) was 0.09 – 0.38 ppm. The median precision of GasFinder devices used in this study for 30 min averaged concentration measurements is 0.04 ppm (Häni et al., 2021).

2.2.3. Experimental setup

Based on experimental findings, Harper et al. (2011) advised placing concentration and turbulence measurements at the downwind side of the housing at a distance of at least 10 times the maximum building height so that the devices are outside the disturbed turbulence field. For the present site this corresponds to a distance of 85 m. From previous wind measurements at the site, two distinct main wind sectors, northeast and southwest had been identified (Fig. 1). Towards northeast, GasFinders and the sonic anemometer (Gill Windmaster, Gill Instrument Ltd., Lymington, UK) were placed at a distance of at least 120 m. Towards southwest, however, the instruments had to be placed at a shorter distance of at least 60 m (Fig. 1) due to a main road passing on this side of the housing.

On the northeast side two GasFinders with a path length of 50 m and 42 m were placed next to each other. The average heights of the measuring paths for the two GasFinders were 1.41 m and 1.35 m above ground. These two GasFinders were combined to a single sensor in the bLS simulations to cover a larger fraction of the emission plume and to be less prone to erroneous measurements (Supporting information 1). For the intervals where only one of the devices passed the quality checks (Section 2.2.2), the emission estimate was based on the measurement of this single sensor only. On the southwest side a single GasFinder was placed with a path length of 75 m with an average height of 1.54 m above ground. At both sides of the dairy housing a 3D sonic anemometer was installed at 1.35 and 1.40 m height (Fig. 1) to derive the turbulence characteristics that are needed as input for the bLS model. Two sonics

Table 1
Herd composition in the first and second campaign (means ± standard deviation).

		Campaign 1	Campaign 2
No of animals per breed	Brown Swiss	27	30
	Swiss Fleckvieh	13	10
No of animals	primiparous	7	11
	multiparous	33	29
Body weight ± 1 SD [kg]		701 ± 82	685 ± 77
Milk yield per day ± 1 SD [kg]		23.2 ± 8.8	25.7 ± 11.0

were used because it was expected to have two dominant wind directions, therefore necessitating two downwind sonics. Sonic measurements were recorded as 10 Hz data in daily files.

The coordinates of the housing and the main GasFinder modules and retroreflectors that were needed to run the bLS model were logged with a handheld global positioning system (Trimble Pro 6T, Trimble Navigation Limited, Sunnyvale, USA). For both campaigns, the GasFinders and sonics were placed at the same location.

2.2.4. Data processing and filtering

The 10 Hz sonic data were corrected for a Gill software bug affecting the magnitude of the vertical wind component (Gill Instruments, 2016). After wind vector rotation (two-axis coordinate rotation), averaged wind and turbulence characteristics for 30 min intervals were calculated. For the evaluation, only the data from the downwind sonic were used. This is more representative as the location coincides with the concentration measurement of the emission plume.

The bLS model is suspected to provide erroneous results given extreme micrometeorological conditions (e.g. very low wind speed, highly unstable or stable conditions). To avoid unrealistic and error-prone emission results, the data were quality filtered (e.g Flesch et al., 2005; Flesch et al., 2018). Filters were applied for the friction velocity (u^*), the Obukohv length (L) and the roughness length (z_0). In addition, to exclude periods with instationary wind directions filters for the standard deviation of the along wind divided by u^* (σ_u/u^*), the standard deviation of the crosswind divided by u^* (σ_v/u^*) and the estimated Kolmogorov constant of the Lagrangian structure function ($C0$) were applied. Emission values with either $u^* < 0.05$ m s^{-1}, $|L| < 2$ m, $z_0 > 0.1$ m, $\sigma_u/u^* > 4.5$, $\sigma_v/u^* > 4.5$, $C0 > 10$ were removed. Additionally, the data were filtered for wind direction. Wind direction filtering is done to make sure that most of the plume from the source is caught by the line-integrating concentration measurements. More information on wind direction filtering is given in the Supporting information 3. Data from measurement intervals which coincided with processes of the slurry pit (e.g. emptying cross channels, slurry agitation) were discarded.

2.2.5. Uncertainty analysis

We estimated the uncertainty ε of the mean IDM emission rate $Q(\Delta t)$ over a certain measurement integration time Δt from the standard deviation SD of consecutive measurement periods of length Δt:

$$\varepsilon_Q(\Delta t) = 2 \cdot \mathrm{SD}\left\{\overline{Q}_i(\Delta t)\right\} \tag{3}$$

ε_Q was analysed for time periods Δt of increasing length (effective measurement time without data gaps). This was done with the data set of the first campaign as it is longer and has less gaps than the second campaign. For practical reasons, the data set was truncated to 360 h and Eq. 3 was evaluated for $\overline{Q}_i$ averaged over time periods between 1 h and 45 h. ε_Q corresponds to a 95% confidence interval of the respective mean under the ideal assumption of a constant Q with time. Since the calculated SD may also include true variations of Q, ε_Q is considered as an upper boundary estimate for the uncertainty of the mean emission.

To estimate the IDM measurement time length, which is necessary to determine the mean emission rate $\overline{Q}$ with a given precision, the results were fitted with a power function of Δt. By extrapolating this function to the total cumulative measurement length of the measurement campaigns, the uncertainty of the mean campaign emissions was estimated.

2.3. Inhouse tracer ratio method

Emissions were measured using a dual tracer ratio method (Schrade et al., 2012) as described in detail by Mohn et al. (2018). The goal of this setup and this housing is to measure two variants in two experimental compartments simultaneously, for comparison as conducted previously by Poteko et al. (2020). The method involves dosing of two different tracer gases, sulphur hexafluoride (SF_6) and trifluoromethyl sulphur pentafluoride (SF_5CF_3), one per compartment, to quantify emissions for each experimental compartment independently and detect potential cross-contamination. Both tracer gases were dosed constantly at floor level using mass flow controllers (Contrec AG, Dietikon, Switzerland) to regulate the total flow and critical steel orifices to achieve homogenous spatial distribution. Representative air sampling in each compartment was accomplished with critical glass orifices (250 µm in diameter 2.5 m above the ground; Thermo-Instruments, Dortmund, Germany, and Louwers, Hapert, The Netherlands). Concentrations of the tracer gases and CH_4 were analysed in real time by gas chromatography with electron capture detection (GC-ECD, model 7890A, Agilent Technologies AG, Basel, Switzerland) and by cavity ring-down spectrometer (CRDS, model G2301, Picarro Inc., Santa Clara, USA).

The quantification of emissions with the tracer ratio method is based on the assumption that the tracer gas (SF_6, SF_5CF_3) behaves in the same way as the target gas and thus mimics the emitting source (Demmers et al., 2001). The mass flow of the target gas ($\dot{m}_{target}$) is calculated from the ratio of the background corrected target (c_{target}) and tracer gas concentration (c_{tracer}) and the mass flow of the tracer gas ($\dot{m}_{tracer}$) as given in Eq. 4:

$$\dot{m}_{target} = \frac{\dot{m}_{tracer} * \ C_{target}}{C_{tracer}} \tag{4}$$

Background concentration was sampled at a point situated at 30 m southeast of the building (Fig. 1). More details on the implemented analytical technique and its performance with respect to suitability for point/areal sources, sensitivity, and uncertainty have been described in Mohn et al. (2018). In the study of Mohn et al. (2018), with constant CH_4 dosing through critical orifices, the absolute uncertainty of the iTRM was reported to be better than 10% for daily averages.

The applied measurement sequence provided emission data with a temporal resolution of 10 min per compartment. To make the iTRM data comparable to the IDM data, 30 min averages for each experimental compartment were calculated and afterwards both compartments summed up. Milking times were excluded from the iTRM analysis, as no animals or only parts of the herd were present in the experimental compartments during these periods.

2.4. Comparison with iTRM emissions

The iTRM measurements were running only during certain times of the IDM campaigns (Section 2.1.3). To make a valid comparison, only 30 min measurement intervals where both methods provided valid data were considered. Based on those data pairs, the average CH_4 emissions of IDM and iTRM were calculated separately for campaign 1 and campaign 2. For this purpose, the data were not weighted e.g. in relation to hour of the day or micrometeorological conditions.

The experimental site comprises two CH_4 sources, the dairy housing and the adjacent slurry pit (Fig. 1), with the second expected to have a much lower emission strength (Petersen, 2018). It can be assumed that measurements of the iTRM do not capture emissions from the slurry pit. Thus, for comparison of CH_4 emissions by IDM and iTRM, the emissions from the slurry pit were subtracted from the total IDM emissions. This correction and the assumptions used to estimate emissions from slurry storage are described in detail in the Supporting information 2. If not otherwise noted, CH_4 emissions are given without the slurry pit.

3. Results

3.1. Meteorological conditions

The average temperature during campaign 1 and campaign 2 was 12.3 °C and 3.4 °C, respectively. The predominant wind directions were southwest (around 233°) and northeast (around 60°) during both

campaigns. Wind speeds were mostly below 2 m s^{-1}, with occasional periods with higher wind speeds (Fig. 2).

The diurnal pattern observed for the wind direction resembles a mountain-valley wind system. This means that there is wind during the day from one direction and during the night from the opposite direction. For this site, there was predominantly northeasterly wind and unstable atmospheric conditions at day and southwesterly wind and stable conditions at night. The diurnal pattern is more distinct in the first than in the second campaign. During the second campaign, periods prevailed over several days with wind from one direction and the mountain-valley like wind system was only observed occasionally (Fig. 2).

3.2. Quality selected IDM emissions

Fig. 3 shows the percentage of data loss for both IDM campaigns as a function of time of day. In campaign 1, the data loss was largest in the morning and evening, while in campaign 2, the proportion of data loss was largest during the night. In total, there are 745 and 448 valid half-hourly IDM emission intervals for the first and second measurement campaign, respectively. This corresponds to a data loss of 57% and 64% (average 60%) due to quality filtering and failure of the GasFinders for the first and second campaign, respectively.

Fig. 4 displays the filtered IDM CH_4 emission data for campaign 1 and campaign 2. The subperiods, during which parallel measurements with the iTRM were conducted, are highlighted by orange shaded areas. Valid data were obtained throughout the entire duration of the measurement campaigns with larger data gaps (Fig. 4) due to mostly GasFinder measurement failure. The main reasons for the larger data loss in campaign 2 was displacement of the GasFinders due to unstable mounting on the wet soil or impacts of wind, resulting in a misalignment of the laser beam of the GasFinders. The data loss in the morning and evening hours of campaign 1 coincided with instationary time periods where the wind direction changed from southwest to northeast and vice versa. Data loss in the second campaign was largest during the night.

As the number of 30 min intervals with valid IDM CH_4 emission data varies over the course of the day, the data were first averaged within groups of equal 'hour of day' values before calculating the overall average. This resulted in daily-average CH_4 IDM emission estimates for the first campaign and second campaign of 0.74 (±0.10) kg h^{-1} and 0.61 (±0.10) kg h^{-1}, respectively. The uncertainty is given as 95% confidence interval derived according to Section 2.2.5. The relative uncertainty for the first and second campaign is 14% and 16%, respectively. For comparison with literature data, daily average emissions were scaled to LU (Livestock Unit with 500 kg live weight) with the live weight given in Table 1. For the first and second campaign, the resulting CH_4 emissions by IDM were 317 (±44) g LU^{-1} d^{-1} and 267 (±43) g LU^{-1} d^{-1}, respectively.

If the emissions from the slurry pits are included, the resulting CH_4 emissions by IDM for the first and second campaign were 342 (±48) g LU^{-1} d^{-1} and 269 (±43) g LU^{-1} d^{-1}, respectively.

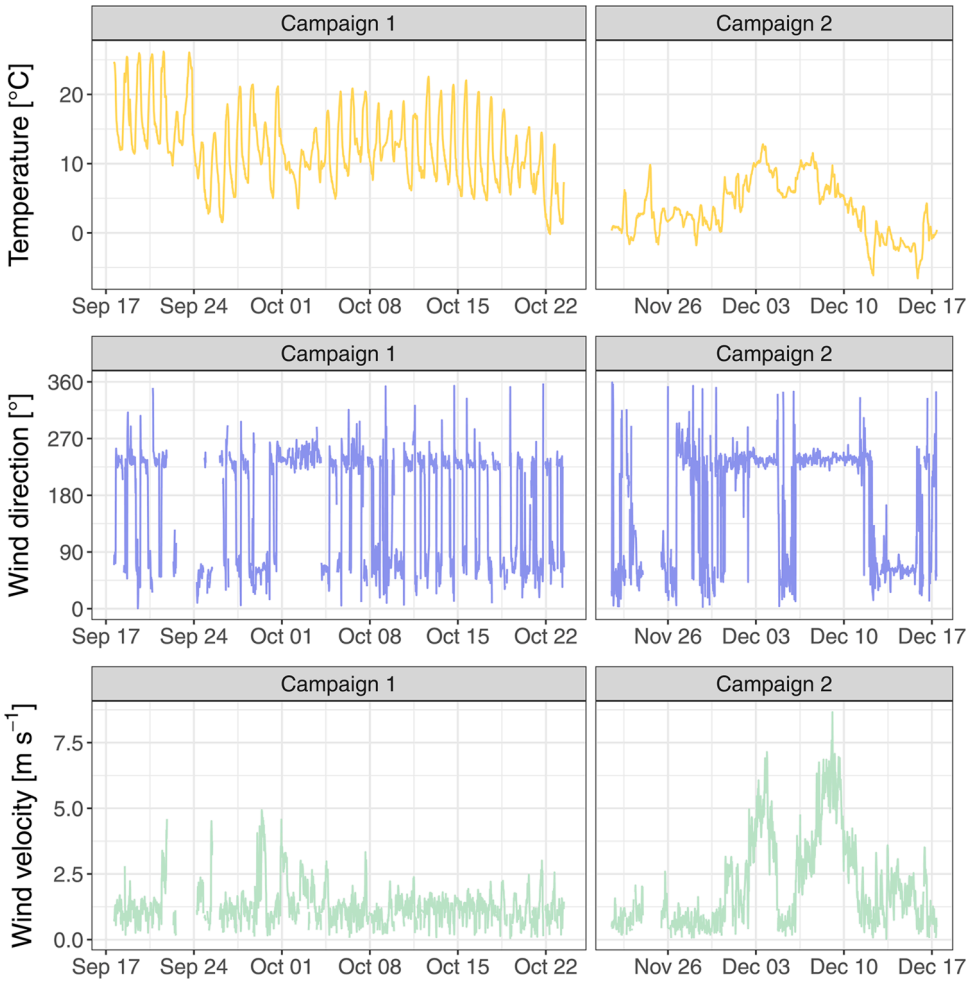

Fig. 2. Meteorological conditions during campaign 1 and campaign 2: temperature (upper panel), wind direction (mid panel) and wind velocity (lower panel). The temperature was recorded at the MeteoSwiss weather station in Tänikon. The wind direction and wind speed were taken from the upwind sonic anemometer at the measuring site.

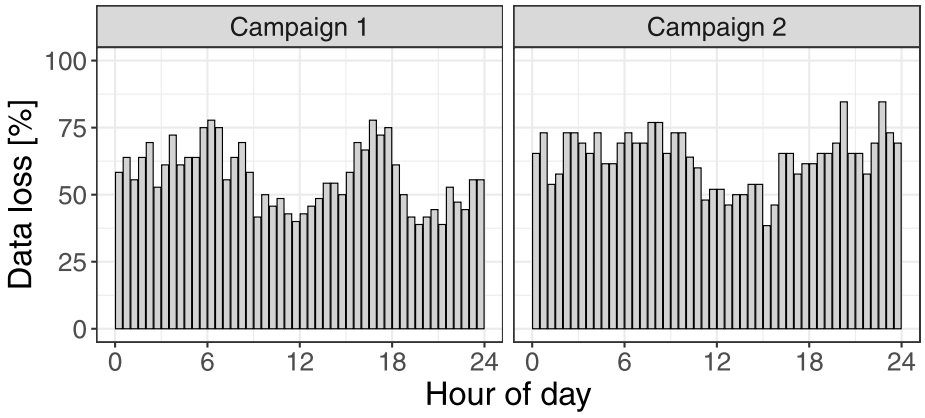

Fig. 3. Data loss of quality filtered IDM emission data as function of hour of day for the two campaigns. Lower values mean more valid data.

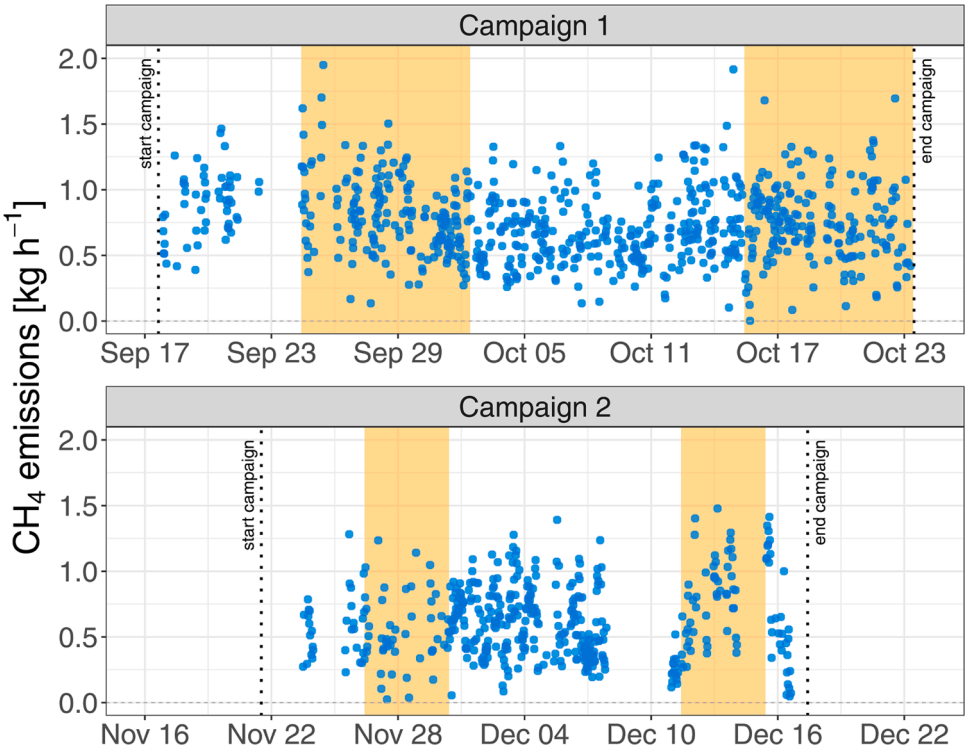

Fig. 4. Half-hourly CH_4 emissions of the dairy housing determined by IDM for campaign 1 (upper panel) and campaign 2 (lower panel). Displayed data are quality filtered. The subperiods with simultaneous iTRM measurements are marked as orange shaded areas.

3.3. Dependence on micrometeorological conditions and diurnal variation

In the first campaign during the day (07:30 – 16:30), there were mostly unstable conditions and northeast wind. During the night (16:30 – 07:30), stable conditions and southwest wind with on average slightly lower friction velocity than during the day prevailed. In campaign 1, the mean CH_4 emission, determined with the IDM, for northeast wind was 4% lower than for southwest wind. For stable conditions the CH_4 emission was 6% lower than with unstable conditions. A correlation between the atmospheric stability, represented by the Obukhov length L, and wind direction in the first campaign is discernable (Fig. 5). The algebraic sign of L is given by the sensible surface heat flux. For convective or unstable conditions (typically during the day) the surface heat flux is positive and hence $L < 0$. For stable conditions the surface heat flux is negative and hence $L > 0$. If $|L| \to \infty$ then $L^{-1} \to 0$ which are neutral conditions (Monin and Obukhov, 1954).

In the second campaign, the distribution of stability, wind direction and friction velocity are very similar during the day and night. In campaign 2 the mean CH_4 emission was 18% lower for southwest wind than for northeast. For stable conditions the CH_4 emission was 9% lower than with unstable conditions. The differences in CH_4 emission in either campaign for wind direction or atmospheric stability are within the standard deviation and the approximated uncertainty of the emissions.

The diurnal variations of CH_4 emission, housing temperature (average of the two compartments) which is proportional to ambient temperature and wind speed recorded at the downwind sonic, are plotted as hourly averaged boxplots (Fig. 6). Temperature and wind speed values are shown for corresponding intervals with a valid emission number. In campaign 1, highest emissions were observed between 8:30 and 13:30 and smallest emission are visible around 3:30 and 15:30. In campaign 2, emission minima occur around 5:00 and 17:00. From 6:00 to 16:00 and 18:00 to 20:00, the emissions are slightly higher than

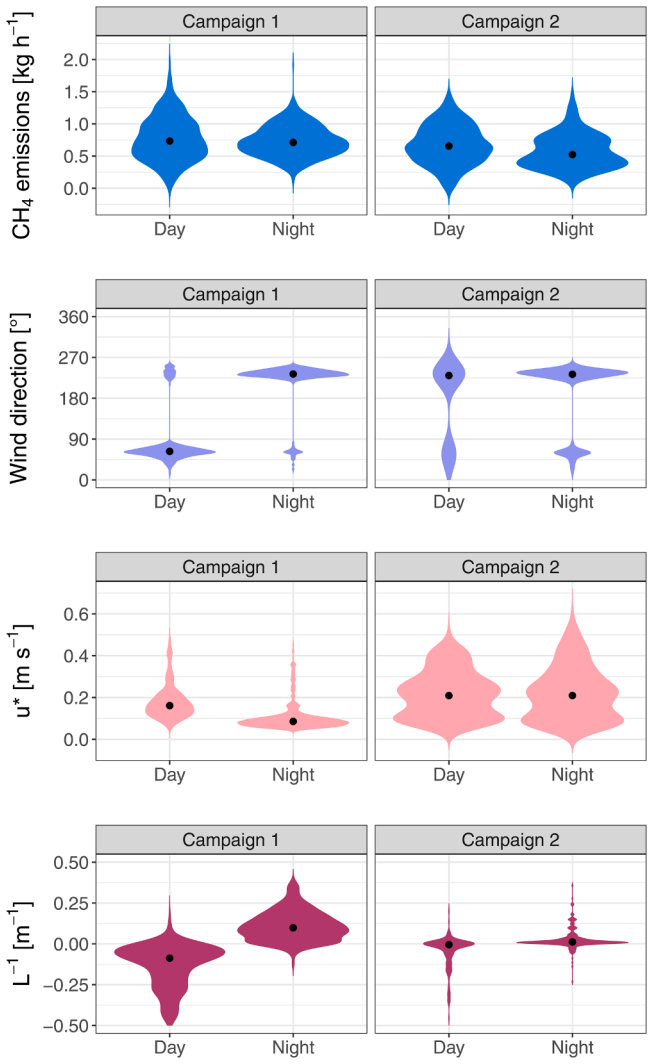

Fig. 5. Violine plots for CH_4 IDM emission (fist panel), wind direction (second panel), friction velocity u^* (third panel) and the inverse of the Obukhov length L (last panel) differentiated by day (07:30–16:30) and night (16:30–07:30) local time for both campaigns. The black dot indicates the median.

at other times. The temperature in the first campaign was lowest around 6:00 and highest at 14:30, whereas in the second campaign the temperature remained constant during the day. In the first campaign, wind speed was increasing from 10:00 onwards and decreases after 15:00 again. In the second campaign, highest wind speeds were recorded around 6:00 but the variation was high throughout the day.

3.4. Comparison with iTRM emission

Fig. 7 shows the scatterplot of CH_4 emission data, where simultaneous IDM and iTRM measurements were available. The variation in the IDM emission data is somewhat larger than that of the iTRM emissions and the correlation between the two methods is 0.02.

In campaign 1 and campaign 2, there are 324 and 90 data pairs derived from the IDM and the independent ITRM measurements, respectively, with valid simultaneous half-hourly data (Table 2). For this subset of data, the iTRM emissions exceeded the IDM results by 0.06 kg h^{-1} and 0.01 kg h^{-1} (or 8% and 1%), for the first and second campaign, respectively. The uncertainty for the average IDM emission (Section 2.2.5), in the first and second campaign is 0.14 and 0.17 kg h^{-1}, respectively. For iTRM the uncertainty is 0.09 and 0.07 kg h^{-1} for the first and second campaign, respectively (Section 2.4). The differences in average emission for the two methods are within the uncertainty of both methods.

4. Discussion

4.1. IDM emission estimates

The average emissions determined by IDM agree, within their uncertainty range of 18-24%, with the emissions simultaneously determined by the fully independent iTRM (Table 2). The iTRM that has been installed in the dairy housing earlier is considered a good candidate for a reference method (Ogink et al., 2013). In a previous validation study, with constant CH_4 dosing through critical orifices, the absolute uncertainty of the iTRM was reported to be below 10% (Mohn et al., 2018), which is lower than that of IDM. Therefore, the good agreement of both methods indicates that the IDM achieved a good accuracy for average CH_4 emissions in the present study.

The mean emissions per LU obtained in this study of 317 (±44) g LU^{-1} d^{-1} and 267 (±43) g LU^{-1} d^{-1} for the first and second campaign, respectively, lie within the range of other published studies. Poteko et al. (2020) reported an emission of 327 g LU^{-1} d^{-1} based on measured emissions from dairy cows in respiration chambers. Hempel et al. (2020) investigated two naturally ventilated dairy cattle buildings and obtained mean CH_4 emissions of 276 g LU^{-1} d^{-1} and 340 g LU^{-1} d^{-1}, respectively. Schmithausen et al. (2018) determined emissions between 225 and 307 g LU^{-1} d^{-1} for a naturally ventilated dairy cattle housing. Both studies investigated systems with loose housings and cubicles, solid or slatted floors and applied a CO_2 mass balance method. In summary, we conclude that the average IDM CH_4 emissions agree well with both, the independent iTRM measurements and the literature.

4.2. Factors influencing IDM emissions

At the measurement site, the dairy housing causes a disturbance of the wind field. The induced disturbance conflicts with the requirements of the bLS model that assumes a horizontally homogeneous wind field. To keep errors small due to such a disturbance, the sonics and GasFinders should to be placed at a minimum distance of about ten times the maximal building height downwind of the source as suggested by Harper et al. (2011). On the northeast side the minimal distance of the measuring path to the dairy housing was 120 m. With a maximum building height of 8.5 m the distance between the GasFinders and the housing was thus sufficient. On the southwest side the minimal distance was only 60 m due to the nearby main road and thus rather close to the housing (Fig. 1). Average emissions for the two wind directions and two stabilities lie within the uncertainty range of the measurements. Thus, we conclude that the measurement fetch did not cause a detectable difference in the measured CH_4 emissions. Nevertheless, there is a distinction between the measurement with southwest and northeast wind which could be due to the difference in the distance to the building (Supporting information 4).

In the first campaign, there is a distinct diurnal cycle of the housing temperature that follows the ambient temperature. For wind speed, a small diurnal cycle with higher values during the day is discernable. For the CH_4 emissions however, no diurnal cycle was detected. There is a decrease in emissions from midnight towards early morning and then slightly higher emissions until the afternoon. However, the boxplots in Fig. 6 show a large variation. In the second campaign, there is almost no variation in wind speed and housing temperature, but the emissions are slightly higher during the day. No systematic dependency of the CH_4 emissions on temperature or wind speed was detected as they are either phase shifted (first campaign) or are constant at varying CH_4 emissions (second campaign). In contrast to our study, Hempel et al. (2020) found a minimum in the CH_4 emissions for temperatures at around 10 °C to 15 °C. Poteko et al. (2020) observed a diurnal cycle in the CH_4 emissions with a peak in the evening after the second milking. Felber et al. (2015)

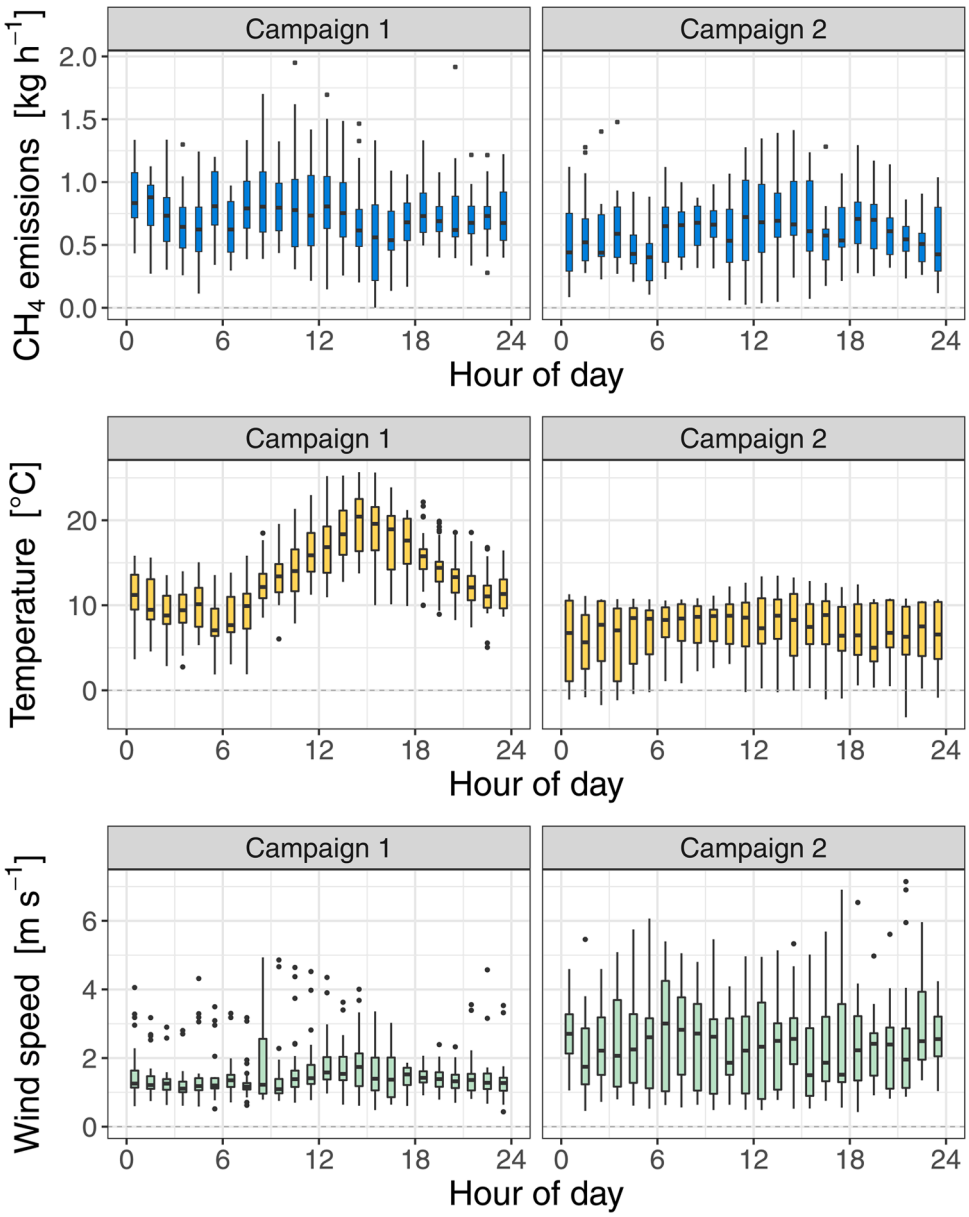

Fig. 6. Average diurnal variation of CH_4 emission (upper panel), average housing temperature of the two compartments (mid panel) and wind speed at the downwind sonic (lower panel) plotted as hourly boxplots.

observed a similar pattern where the maximum emission in the evening coincided with the most distinct grazing activity. The studies of Hammond et al. (2016) and Poteko et al. (2020) suggest that such high CH_4 emissions are associated with feeding. On the other hand, Laubach et al. (2014) and McGinn et al. (2011) observed higher emissions during day for grazing cattle. Overall, the studies provided diverse diurnal emission patterns.

Four our study, we cannot rule out that the observed variation in IDM CH_4 emission data may be mainly controlled by the temporal fluctuations (within precision levels) in the concentration measurements. The median (and respective interquartile range) of the measured concentration difference ΔC between the up- and downwind GasFinder was 0.18 ppm (0.09–0.40 ppm). For the GasFinders used in this study (all of them were also used in the study of Häni et al. (2021)), the median precision for one 30 min measurement is 0.04 ppm. This corresponds to a median uncertainty in the concentration measurements of 22%.

We conclude that the variation in the real CH_4 emission were smaller than the modulation of the IDM calculations through other influences (e.g. concentration measurements, deviations of bLS model from reality, diurnal cycle associated with feeding). This is supported by the lacking correlation between the half-hourly results of both measurement methods IDM and iTRM (Fig. 7) which could be due to uncertainty in either or both methods. For IDM, we assume the factor dominating temporal variability was the CH_4 analytics because concentrations measured downwind were close to ambient levels and thus more affected by the precision of the GasFinder analysers.

4.3. Uncertainty analysis

The uncertainty of the average IDM emissions (calculated according to Eq. 3) depends on the averaging period Δt. This relationship is plotted in Fig. 8. Instead of the absolute uncertainty, the relative uncertainty $(\varepsilon / \overline{Q})$ is used here.

The more measurement intervals are included for the calculation of the mean emission the smaller the relative uncertainty gets. We have an average data loss of 60% in this study, which is in the range of other

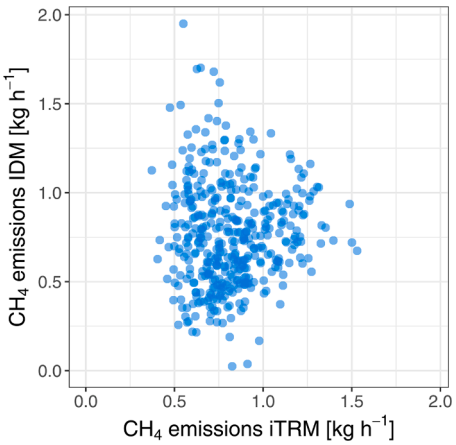

Fig. 7. Scatterplot of CH_4 30min emission data for both campaigns, where simultaneous and valid measurement data for both IDM and iTRM method are available.

Table 2
Number of valid data pairs and average CH_4 emissions and standard deviation (in parentheses) for time intervals with simultaneous IDM and iTRM measurements, specified for both campaigns.

	Campaign 1	Campaign 2
Number of valid data pairs	324	90
Average CH_4 emissions IDM [kg h^{-1}]	0.79 (0.28)	0.69 (0.31)
Average CH_4 emissions iTRM [kg h^{-1}]	0.85 (0.22)	0.70 (0.12)

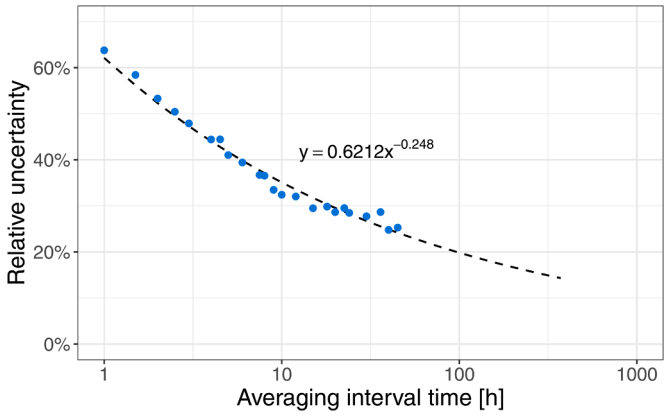

Fig. 8. Relative uncertainty of the mean emission given for different averaging intervals according to Eq. 3. The dotted line indicates the fitted power law. Note that the x-axis has a logarithmic scaling.

studies reporting between 50% and 90% periods of time with invalid data (Flesch et al., 2014; VanderZaag et al., 2014). More important, we obtained sufficient observations throughout 24 h of the day (Fig. 3). With the power function given in Fig. 8 and assuming a constant emission it is possible to calculate the minimum needed effective measuring time to reach a certain uncertainty. For e.g. 20% uncertainty this would be 96 h. Accounting for a data loss of about 60%, a measurement period of about 10 days is thus necessary. We recommend measuring beyond 10 consecutive days to obtain data under different micrometeorological conditions and to have a sufficient safety margin in case of larger data loss.

5. Conclusions

The CH_4 emissions from a small dairy housing with 40 lactating cows measured with IDM are in good agreement with the simultaneously determined iTRM emissions. The differences are within the uncertainty of either of the two methods. The emission factors per LU from this study agree well with the range of other studies. The findings suggest that the bLS model is not affected by external parameters like stability, friction velocity or temperature at this site with difficult micrometeorological conditions. Unlike other studies, no clear diurnal cycle in the CH_4 emissions was detected. However, it is possible that the different factors influencing the emission determination (wind direction, stability, feeding) cancel each other out which could induce the observed constant emissions patterns or temporal changes might be masked by the limited precision of the analysers. To disentangle these effects and identify shortcomings of any or both methods (IDM, iTRM), an optimised experimental design and extended measurements would be required. For IDM, we suggest an experiment with controlled artificial release of CH_4 well above ambient concentrations within an empty dairy housing and concentration measurements at several distances downwind of the source to determine the recovery rate at each distance under stable and unstable conditions and different u^* values.

Declaration of Competing Interest

The authors declare that they have no known competing financial interests or personal relationships that could have appeared to influence the work reported in this paper.

Acknowledgments

Funding by the Swiss Federal Office for the Environment (Contract 00.5082.P2I R254-0652) is gratefully acknowledged. We thank Markus Jocher (Climate and Agriculture Group, Agroscope, Zürich) for supporting the operation of the measurement devices and gratefully acknowledge the contribution of Michael Döring (Niels Bohr Institute, University of Copenhagen) to the manuscript. We are grateful to the support and assistance of the following persons involved in the experiment: M. Keller, M. Hatt, T. Kupferschmid (Agroscope Tänikon), S.A. Wyss (Empa Dübendorf) and the farmer of the land in the surrounding area of the experimental housing, W. Denzler.

Supplementary materials

Supplementary material associated with this article can be found, in the online version, at doi:10.1016/j.agrformet.2021.108501.

References

Bai, M., Sun, J., Denmead, O.T., Chen, D., 2017. Comparing emissions from a cattle pen as measured by two micrometeorological techniques. Environ. Pollut. 230, 584–588.
Boreal Laser Inc., 2018. GasFinder3-OP Operation Manual. Part No. NDC-200036.
Demmers, T., Phillips, V.R., Short, L.S., Burgess, L.R., Hoxey, R.P., Wathes, C.M., 2001. SE—Structure and environment: Validation of ventilation rate measurement methods and the ammonia emission from naturally ventilated dairy and beef buildings in the United Kingdom. J. Agric. Eng. Res. 79 (1), 107–116.
Federal Statistical Office, 2020. Agriculture and food: Pocket statistics 2020. Agriculture and forestry 07. Federal Statistical Office, Neuchâtel, Switzerland.
Felber, R., Münger, A., Neftel, A., Ammann, C., 2015. Eddy covariance methane flux measurements over a grazed pasture: effect of cows as moving point sources. Biogeosciences 12 (12), 3925–3940.
Flesch, T.K., Basarab, J.A., Baron, V.S., Wilson, J.D., Hu, N., Tomkins, N.W., Ohama, A.J., 2018. Methane emissions from cattle grazing under diverse conditions: an examination of field configurations appropriate for line-averaging sensors. Agric. For. Meteorol. 258, 8–17.
Flesch, T.K., Harper, L.A., Powell, J.M., Wilson, J.D., 2009. Inverse-dispersion calculation of ammonia emissions from Wisconsin dairy farms. Trans. ASABE 52 (1), 253–265.
Flesch, T.K., McGinn, S.M., Chen, D., Wilson, J.D., Desjardins, R.L., 2014. Data filtering for inverse dispersion emission calculations. Agric. For. Meteorol. 198-199, 1–6.
Flesch, T.K., Vergé, X.P.C., Desjardins, R.L., Worth, D., 2013. Methane emissions from a swine manure tank in western Canada. Can. J. Anim. Sci. 93 (1), 159–169.
Flesch, T.K., Wilson, J.D., Harper, L.A., Crenna, B.P., 2005. Estimating gas emissions from a farm with an inverse-dispersion technique. Atmos. Environ. 39 (27), 4863–4874.

Flesch, T.K., Wilson, J.D., Harper, L.A., Crenna, B.P., Sharpe, R.R., 2004. Deducing ground-to-air emissions from observed trace gas concentrations: a field trial. J. Appl. Meteorol. 43 (3), 487–502.
Flesch, T.K., Wilson, J.D., Harper, L.A., Todd, R.W., Cole, N.A., 2007. Determining ammonia emissions from a cattle feedlot with an inverse dispersion technique. Agric. For. Meteorol. 144 (1–2), 139–155.
Gao, Z., Desjardins, R.L., Flesch, T.K., 2010. Assessment of the uncertainty of using an inverse-dispersion technique to measure methane emissions from animals in a barn and in a small pen. Atmos. Environ. 44 (26), 3128–3134.
Gerber, P.J., 2013. Tackling climate change through livestock: A global assessment of emissions and mitigation opportunities. Food and Agriculture Organization of the United Nations FAO, Rome.
Gill Instruments, 2016. Technical key note: Software bug affecting 'w' wind component of the WindMaster family. Gill Instruments, Lymington, UK. http://gillinstruments.com/data/manuals/KN1509_WindMaster_WBug_info.pdf.
Hammond, K.J., Crompton, L.A., Bannink, A., Dijkstra, J., Yáñez-Ruiz, D.R., O'Kiely, P., Kebreab, E., Eugène, M.A., Yu, Z., Shingfield, K.J., Schwarm, A., Hristov, A.N., Reynolds, C.K., 2016. Review of current in vivo measurement techniques for quantifying enteric methane emission from ruminants. Anim. Feed Sci. Technol. 219, 13–30.
Häni, C., Bühler, M., Neftel, A., Ammann, C., Kupper, T., 2021. Performance of open-path GasFinder3 devices for CH_4 concentration measurements close to ambient levels. Atmos. Meas. Tech. 14 (2), 1733–1741.
Häni, C., Flechard, C., Neftel, A., Sintermann, J., Kupper, T., 2018. Accounting for field-scale dry deposition in backward Lagrangian stochastic dispersion modelling of NH_3 emissions. Atmosphere 9 (4), 146.
Harper, L.A., Denmead, O.T., Flesch, T.K., 2011. Micrometeorological techniques for measurement of enteric greenhouse gas emissions. Anim. Feed Sci. Technol. 166-167, 227–239.
Harper, L.A., Flesch, T.K., Wilson, J.D., 2010. Ammonia emissions from broiler production in the San Joaquin Valley. Poult. Sci. 89 (9), 1802–1814.
Hempel, S., Willink, D., Janke, D., Ammon, C., Amon, B., Amon, T., 2020. Methane emission characteristics of naturally ventilated cattle buildings. Sustainability 12 (10), 4314.
Kupper, T., Bonjour, C., Menzi, H., 2015. Evolution of farm and manure management and their influence on ammonia emissions from agriculture in Switzerland between 1990 and 2010. Atmos. Environ. 103, 215–221.
Laubach, J., Bai, M., Pinares-Patiño, C.S., Phillips, F.A., Naylor, T.A., Molano, G., Cárdenas Rocha, E.A., Griffith, D.W.T., 2013. Accuracy of micrometeorological techniques for detecting a change in methane emissions from a herd of cattle. Agric. For. Meteorol. 176, 50–63.
Laubach, J., Grover, S.P., Pinares-Patiño, C.S., Molano, G., 2014. A micrometeorological technique for detecting small differences in methane emissions from two groups of cattle. Atmos. Environ. 98, 599–606.
McGinn, S.M., Flesch, T.K., Crenna, B.P., Beauchemin, K.A., Coates, T., 2007. Quantifying ammonia emissions from a cattle feedlot using a dispersion model. J. Environ. Qual. 36 (6), 1585–1590.
McGinn, S.M., Flesch, T.K., Harper, L.A., Beauchemin, K.A., 2006. An approach for measuring methane emissions from whole farms. J. Environ. Qual. 35 (1), 14–20.
McGinn, S.M., Janzen, H.H., Coates, T.W., Beauchemin, K.A., Flesch, T.K., 2016. Ammonia emission from a beef cattle feedlot and its local dry deposition and re-emission. J. Environ. Qual. 45 (4), 1178–1185.
McGinn, S.M., Turner, D., Tomkins, N., Charmley, E., Bishop-Hurley, G., Chen, D., 2011. Methane emissions from grazing cattle using point-source dispersion. J. Environ. Qual. 40 (1), 22–27.
Mohn, J., Zeyer, K., Keck, M., Keller, M., Zähner, M., Poteko, J., Emmenegger, L., Schrade, S., 2018. A dual tracer ratio method for comparative emission measurements in an experimental dairy housing. Atmos. Environ. 179, 12–22.
Monin, A.S., Obukhov, A.M., 1954. Basic laws of turbulent mixing in the surface layer of the atmosphere. Contrib. Geophys. Inst. Acad. Sci. USSR 151 (163), e187.
Niu, M., Kebreab, E., Hristov, A.N., Oh, J., Arndt, C., Bannink, A., Bayat, A.R., Brito, A.F., Boland, T., Casper, D., Crompton, L.A., Dijkstra, J., Eugène, M.A., Garnsworthy, P.C., Haque, M.N., Hellwing, A.L.F., Huhtanen, P., Kreuzer, M., Kuhla, B., Lund, P., Madsen, J., Martin, C., McClelland, S.C., McGee, M., Moate, P.J., Muetzel, S., Muñoz, C., O'Kiely, P., Peiren, N., Reynolds, C.K., Schwarm, A., Shingfield, K.J., Storlien, T.M., Weisbjerg, M.R., Yáñez-Ruiz, D.R., Yu, Z., 2018. Prediction of enteric methane production, yield, and intensity in dairy cattle using an intercontinental database. Global Change Biol. 24 (8), 3368–3389.
Ogink, N., Mosquera, J., Calvet, S., Zhang, G., 2013. Methods for measuring gas emissions from naturally ventilated livestock buildings: Developments over the last decade and perspectives for improvement. Biosystems Eng. 116 (3), 297–308.
Petersen, S.O., 2018. Greenhouse gas emissions from liquid dairy manure: Prediction and mitigation. J. Dairy Sci. 101 (7), 6642–6654.
Poteko, J., Schrade, S., Zeyer, K., Mohn, J., Zaehner, M., Zeitz, J.O., Kreuzer, M., Schwarm, A., 2020. Methane emissions and milk fatty acid profiles in dairy cows fed linseed, measured at the group level in a naturally ventilated housing and individually in respiration chambers. Animals 10 (6).
Poteko, J., Zähner, M., Schrade, S., 2019. Effects of housing system, floor type and temperature on ammonia and methane emissions from dairy farming: a meta-analysis. Biosystems Eng. 182, 16–28.
Poteko, J., Zähner, M., Steiner, B., Schrade, S., 2018. Residual soiling mass after dung removal in dairy loose housings: Effect of scraping tool, floor type, dung removal frequency and season. Biosystems Eng. 170, 117–129.
Saunois, M., Stavert, A.R., Poulter, B., Bousquet, P., Canadell, J.G., Jackson, R.B., Raymond, P.A., Dlugokencky, E.J., Houweling, S., Patra, P.K., Ciais, P., Arora, V.K., Bastviken, D., Bergamaschi, P., Blake, D.R., Brailsford, G., Bruhwiler, L., Carlson, K. M., Carrol, M., Castaldi, S., Chandra, N., Crevoisier, C., Crill, P.M., Covey, K., Curry, C.L., Etiope, G., Frankenberg, C., Gedney, N., Hegglin, M.I., Höglund-Isaksson, L., Hugelius, G., Ishizawa, M., Ito, A., Janssens-Maenhout, G., Jensen, K.M., Joos, F., Kleinen, T., Krummel, P.B., Langenfelds, R.L., Laruelle, G.G., Liu, L., Machida, T., Maksyutov, S., McDonald, K.C., McNorton, J., Miller, P.A., Melton, J.R., Morino, I., Müller, J., Murguia-Flores, F., Naik, V., Niwa, Y., Noce, S., O'Doherty, S., Parker, R.J., Peng, C., Peng, S., Peters, G.P., Prigent, C., Prinn, R., Ramonet, M., Regnier, P., Riley, W.J., Rosentreter, J.A., Segers, A., Simpson, I.J., Shi, H., Smith, S. J., Steele, L.P., Thornton, B.F., Tian, H., Tohjima, Y., Tubiello, F.N., Tsuruta, A., Viovy, N., Voulgarakis, A., Weber, T.S., van Weele, M., van der Werf, G.R., Weiss, R. F., Worthy, D., Wunch, D., Yin, Y., Yoshida, Y., Zhang, W., Zhang, Z., Zhao, Y., Zheng, B., Zhu, Q., Zhu, Q., Zhuang, Q., 2020. The Global Methane Budget 2000–2017. Earth Syst. Sci. Data 12 (3), 1561–1623.
Schmithausen, A.J., Schiefler, I., Trimborn, M., Gerlach, K., Südekum, K.-H., Pries, M., Büscher, W., 2018. Quantification of methane and ammonia emissions in a naturally ventilated barn by using defined criteria to calculate emission rates. Animals 8 (5).
Schrade, S., Zeyer, K., Gygax, L., Emmenegger, L., Hartung, E., Keck, M., 2012. Ammonia emissions and emission factors of naturally ventilated dairy housing with solid floors and an outdoor exercise area in Switzerland. Atmos. Environ. 47, 183–194.
Sonderfeld, H., Bösch, H., Jeanjean, A.P.R., Riddick, S.N., Allen, G., Ars, S., Davies, S., Harris, N., Humpage, N., Leigh, R., Pitt, J., 2017. CH_4 emission estimates from an active landfill site inferred from a combined approach of CFD modelling and in situ FTIR measurements. Atmos. Meas. Tech. 10 (10), 3931–3946.
VanderZaag, A.C., Flesch, T.K., Desjardins, R.L., Baldé, H., Wright, T., 2014. Measuring methane emissions from two dairy farms: seasonal and manure-management effects. Agric. For. Meteorol. 194, 259–267.
VanderZaag, A.C., Gordon, R.J., Glass, V.M., Jamieson, R.C., 2008. Floating covers to reduce gas emissions from liquid manure storages: a review. Appl. Eng. Agric. 24 (5), 657–671.